AIAA AVIATION Forum
June 27-July 1, 2022, Chicago, IL & Virtual
AIAA AVIATION 2022 Forum

10.2514/6.2022-3892

An Experimental Investigation on the Aerodynamic and Aeroacoustic Performances of Dual-Rotor Propellers for UAS Applications

Nianhong Han[1], Zicheng Zhang[2], and Hui Hu[3]
Department of Aerospace Engineering, Iowa State University, Ames, IA, 50011-1096, USA

Abstract: Experimental studies were conducted to investigate the aerodynamic and aero-acoustic performance of a dual-rotor configuration applied to small UAVs. The aerodynamic performance, including thrust and power consumption, of a dual-rotor with a contrasting rotationaldirection (anti-rotor) was better than that of a dual-rotor with the same rotational direction (co-rotor), with the thrust of the downstream propeller decreased because of the wake of the upstream propeller. A parametric study with different rotor distances revealed that both the broadband and overall noise of the dual-rotor system increase as rotor distance decreases. In addition to exploring the influence of rotor distance on thrust and noise, this study also used PIV technology to examine flow-field characteristics for different incoming flow velocities.

I. Nomenclature

D = diameter of propeller
S = rotor distance
C_t = thrust coefficient
C_p = power consumption coefficient
J = advanced ration
U = incoming flow velocity
r = span-wise location on propeller
β = position angle relative to upstream propeller
n = rotational speed
ρ = air density
T = thrust
P = power consumption
SLP = Sound pressure level

II. Introduction

With compact design and low cost, unmanned aerial vehicles (UAVs) have become popular and widely-usedplatforms in variety of areas. Since no pilot is required, the design and application of UAVs become extremely flexible, with hundreds of UAV forms developed and applied to different fields [1, 2], including agriculture, the gas andoil industry, urban planning, construction, wildlife conservation, and healthcare. As the most commonly used propulsion solution for small UAVs, due to its vertical take-off and landing capabilities and the hovering and maneuverability, therotary-wing system has attracted considerable attention and further expanded the scope of application of UAVs. Muchwork related the optimization of rotary-wing aerodynamic performance of either has been done or is ongoing [3–7]. To make a UAV more flexible and lighter

[1] PhD Student, Department of Aerospace Engineering.
[2] PhD Student, Department of Aerospace Engineering.
[3] Martin C. Jischke Professor, Department of Aerospace Engineering, AIAA Associate Fellow.

but still able to complete a flight mission in a complex environment, researchersare constantly trying to generate more thrust or to achieve greater effectiveness in limited space to accomplish UAV-basedmissions. In such studies, the dual-rotor(co-axial) configuration has become an effective solution for increasing lift in a limited space [8]. Coaxial-rotor vehicles were initially produced during the early 1900s, but their mechanical complexity tended tomake them less popular than single-rotor vehicles, although theoretical research on dual rotors has continued, with numerous theoretical[9, 10], computational[11], and experimental[12, 13] studies performed over ensuing decades. These studies provide a rich basis for the application of coaxial dual rotors.

To better advance application of small drones, more knowledge is required about optimizing a flow field around low Re coaxial rotors. Some previous simplifying assumptions related to designing large-scale high Reynolds numberdual rotors, such as neglecting viscous effects and assuming thin vortical layers, are no longer suitable when analyzingflow fields of dual rotors under low Reynolds number conditions. Some studies have investigated the aerodynamic performance and flow field of UAV propellers. Hoffmann et al. (2007) [14] showed that fluctuating air speed hasa significant impact on aerodynamic behavior of such propellers, and that total thrust, blade flapping, and airflow disruption will benefit trajectory control. The numerical study of Bristeau et al. (2009) [15]concluded that a quadcopter's dynamics are to a large extent affected by propeller flexibility. Shukle et al. (2019) [8] investigated the low Reynolds number coaxial rotor flow field, including aerodynamic interactions and their effect on rotor performance. Through Stereo Particle Image Velocimetry (SPIV) measurement, better upper rotor performance was achieved through viscousswirl recovery by a counter-rotating lower rotor. Another study by Teys, et al. (2016) [16] investigated the aerodynamicperformance of a dual-rotor configuration using different setups and concluded that propulsion system efficiency wasincreased under high disk-loading conditions. These and many other related studies have been dedicated to investigating and understanding how to optimize the aerodynamic performance of UAV propulsion systems to meet increasingly complex application scenarios in terms of UAV endurance and maneuverability requirements. Taking multi-rotor drones as an example, while it has been shown that multirotor helicopters can reliably fly while completing many types of tasks, flight time is a key issue. For a quadrotor using a 2200mah battery, the mission duration of a multi-rotor helicopter often extends from 7 up to 15 minutes, while a hefty lift using a 5000mah battery generally has a mission requirement of between 15 and 25 minutes. Improving a propeller's aerodynamic power would be an efficient technique for increasingmulti-rotor helicopter flying time, subject to battery and motor restrictions.

On the other hand, with expansion of areas of application, noise has become a key issue for many users[17]. Although in the entire history of aviation development aviation noise has always been a hot issue, the widespread application of drones has brought this issue even closer to people's daily lives. Ditmer, et al(2015)[17] evaluated the impact of UAV flights on heart-rate reactions of free-roaming US black bears, and after observing that all bears in the study responded to UAV flights with heart rate increases as much as 123 beats per minute above the pre-flight baseline, they concluded that it is important to address increased stress on animals from UAV flights when formulating rules and best scientific practices. Some areas have even implemented no-fly measures for drones due to such noise issues.

As the main noise source on UAVs using rotary-wing systems, the rotor itself has become the main object of research related to noise suppression. According to the work of Glegg et al. [18], the noise generated by the propeller can be divided into two main categories: harmonic or narrow-band noise and broadband noise. Harmonic noise is basically the periodic signal caused by periodic propeller rotation, and the main sources of harmonic noise are generally considered to be related to thrust and torque generation, airfoil thickness, and other interaction and distortion effects such as bladeslap, wake-field interaction, etc. The frequency distribution of harmonic noise is closely related to the propeller's rotational frequency. In contrast to harmonic noise, broadband noise is random, non-periodic noise with no obvious frequency-distribution characteristics. The main sources of broadband noise are turbulence and vortex noise producedby a trailing-edge vortex and a wing-tip vortex. Because the generating mechanisms of these two types of noise differ, different methods of suppressing noise have been proposed [19], including optimized geometry, modified wingtip shape, optimizing blade number and blade distribution, etc.

With the recent rapid growth of the UAV market, methods to reduce noise generated by UAV propellers have been proposed. Ning et al.[20] investigated the effect of a serrated trailing-edge propeller. By measuring

the aero-acoustic performance and the flow field, this study concluded that a saw-tooth serrated trailing edge could reduce broadband noise. The same group also studied about bio -inspired propeller [21],in which a propeller design based on a maple-seed shape was proposed and proved through experiments that it produced greater noise suppression than a baseline propeller generating the same thrust. Leslie et al. [22] studied applying a leading-edge boundary-layer strip to achieve suppression of broadband noise level. They concluded that both the serrated strip and the straight strip produced noise suppression. In this study, an experimental investigation was conducted to examine the influence of the distance between the dual rotors on the noise level, combines research on dual-rotor flow field and noise performance.

III. Experiment setup

The aerodynamic performance measurement and aeroacoustic investigation were separately conducted. The first part ofthe experiment, to investigate the aerodynamic performance of the dual-rotor system, was performed in a low-speed wind tunnel available at Iowa State University. The wind tunnel could achieve wind velocity up to 50m/s with turbulence intensity less than 0.003, and two separate force&torque transducers were used to quantify the thrust generated by each propeller. A high-resolution particle-imaging velocimetry (PIV) system was also used to inspect the flow field around the dual-rotor system and the distribution, spread, and interaction of vortices. A parametric study was conducted for different rotor distances and incoming flow velocities. To achieve better understanding of the aerodynamic and aero-acoustical performance characteristics of a dual-rotor system compared to one with a single rotor, the experimentwas performed with both an anti-rotating dual-rotor and a co-rotating dual-rotor.

The next phase of the experiment was carried out in an anechoic chamber located in the Iowa State University's Aerospace Engineering Department. The noise generated by the dual-rotor system at different positions along the circumferential direction was measured using acoustic microphones. The time-domain noise signal sequence was thenconverted into a frequency-domain signal using fast Fourier transformation. A parametric study was then performed toinvestigate the effect on the noise level of the dual-rotor system of distance between the two rotors.

A. Experiment setup for flow field investigation

A schematic diagram of the experimental setup for flow field and aerodynamic investigation is shown in Figure1. Upstream and downstream propellers were separately connected to the wind-tunnel ceiling through ATI mini45 force&torque transducer separately. Both propellers were of type DJI 9443, an off-the-shelf and widely-used model invarious kinds of multi-rotors. Figure2 shows a propeller image and the Reynolds number distribution in the span-wisedirection when the rotational speed was 5000 rpm. The suction side of each of the two propellers both faced the incoming flow, and the distance between the two propellers S was adjustable. Two laser-based tachometers were connected to PID controllers to separately maintain the rotational speeds of the two propellers. The propellers were mounted on brushless motors controlled by electric speed controllers, and Hall current sensors were used to measure the current input to each motor. A DC power supply was used to provide 12V power. The motor drive and control system similar to the description in the work of Han et al. [23].

A laser transmitter placed under the wind tunnel emitted a laser sheet passing through the center of rotation of thetwo propellers in the vertical direction. Because the flow field to be explored was relatively long in the horizontal direction, two high-speed cameras are used in the experiment to ensure sufficient resolution. These two PCO-1600 cameras were placed side-by-side horizontally, with the focal plane coinciding with the laser plane. The two cameraswere synchronously triggered, and the acquired images stitched together through post-processing.

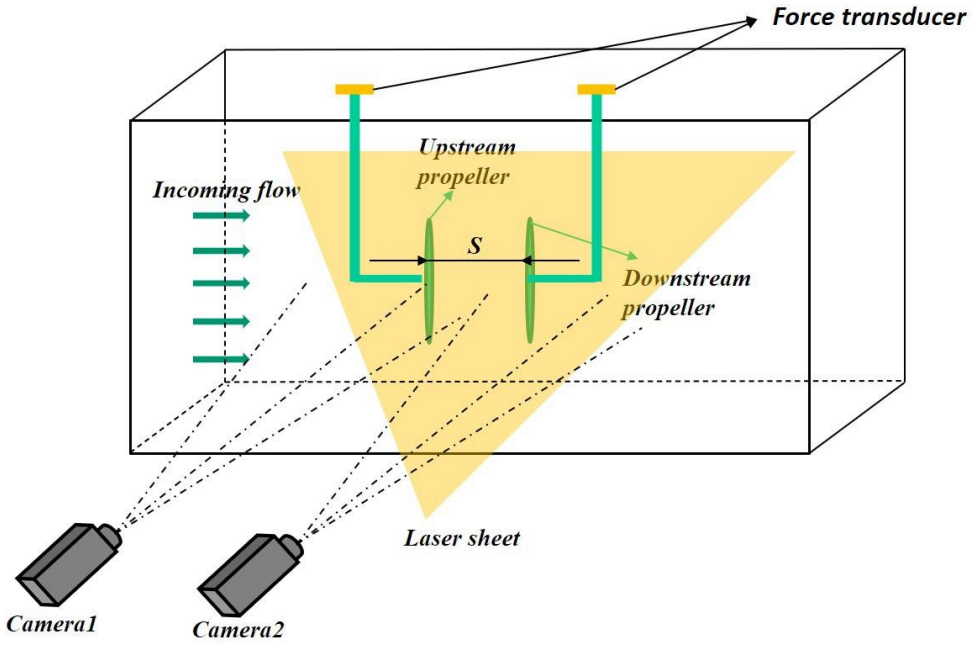

Fig. 1: Experiment set up of flow field measurement using PIV system

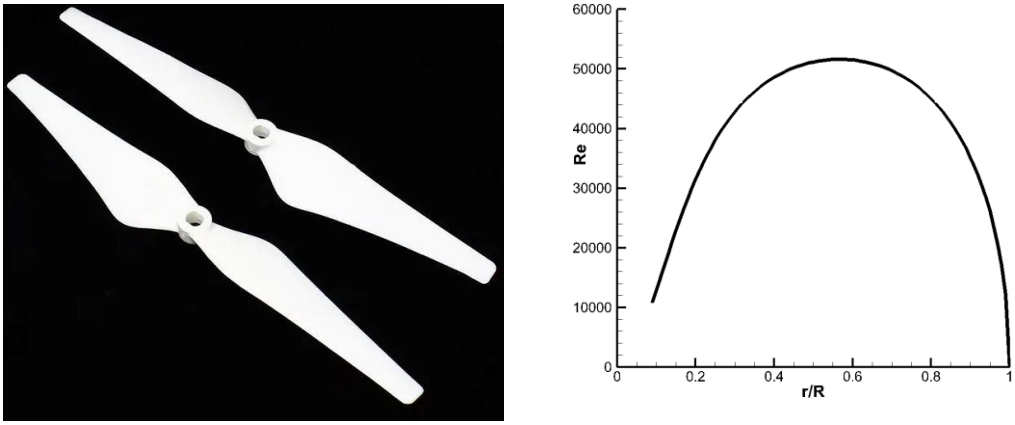

(a).9443 propeller (b) Reynolds number distribution along blade span

Fig. 2 Propeller used in the experiment and the local Reynolds number distribution along span-wise directionwith 5000rpm rotational speed

B. Experiment setup for aero-acoustical performance investigation

The aero-acoustic experiment was performed in an anechoic chamber located in the Iowa State University Department of Aerospace Engineering. The chamber size was 12 x 12 x 9 feet and it had a 100 Hz cut-off frequency. The dual-rotorsystem was placed at the center of the chamber. With the rotational center of the upstream propeller taken as the center of the circle, and the direction back to the airflow direction of the propeller and perpendicular to the rotation plane taken as the 0-degree position angle, β, the microphone was placed at 5 different position angles (β = 0°, 30°, 60°, 90°, 150°) at distance 5D (1 rotor diameter =240mm) from the center. This setup was similar that used by Ning et al. (2016). The 5D measurement distance was chosen to avoid interference from the near-field flow field, usually within 2D. The highturbulence level in the near field would affect the sound measurement. The downstream propeller was adjustable, and the rotor distance S was changed from 0.2D to 1.4D (S = 0.2D, 0.4D, 0.6D, 0.8D, 1.0D,

1.2*D*). The experimental setup is shown in Figure3. The noise generated by the dual-rotor system at different positions along the circumferential direction was measured by a PCB 130D20 acoustic microphone whose frequency response (-2 to +5 dB) was from 20Hz to 15000Hz with a sensitivity of 45 *mV/ Pa* (-26.9*dBV*). A data-acquisition system was used to record the noise signal at a frequency of 50,000Hz. The time-domain noise signal was divided into 50 segments for fast Fourier transformation, producing the averaged frequency-domain noise signal distribution. All signals were processed using Hanning window functions.

C. Test Conditions

The test conditions for aerodynamic performance and flow field measurement are shown in Table1. For comparison,a group of propellers with opposite rotating directions (anti-rotor) and a group of propellers with the same rotating direction (co-rotor) were tested with the same upstream propeller and a reversed downstream propeller. The incomingflow velocity was varied from 0 to 6m/s, corresponding to hovering and take-off or vertical climbing situation. For a parametric study, the rotor distance changes were changed from 0.2D to 1.2D, with the system input voltage maintainedas 12 volt, so the current sensor represented the change in power consumption.

For the aero-acoustic measurement, only the anti-rotor configuration was investigated, with propeller driving systems the same as described above. Since the test facility cannot provide incoming flow, all the tests were made to reflect ahovering situation.

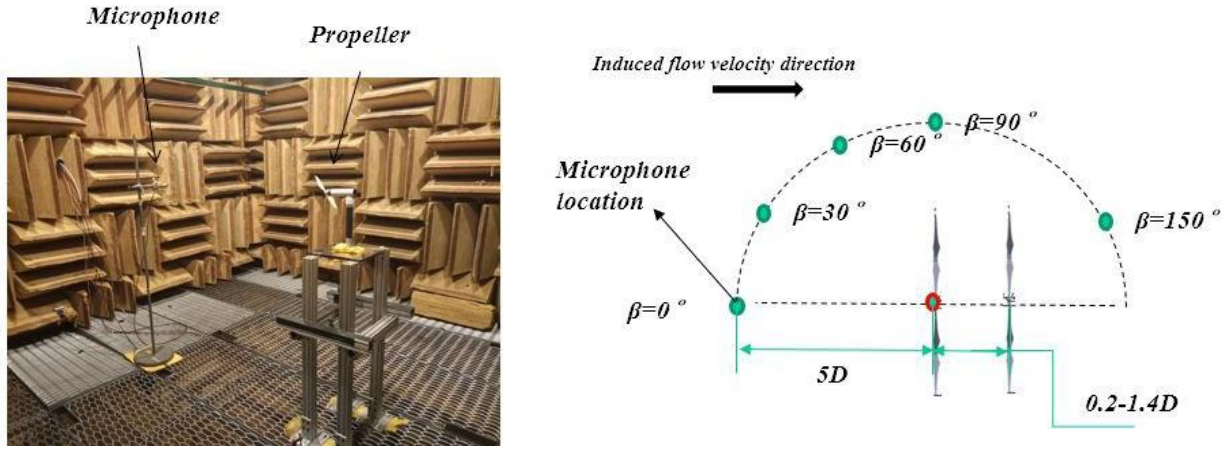

(a) Experiment setup in the anechoic chamber (b) Distribution of Measurement position

Fig. 3 Experiment set up of noise measurement

Table 1. Test condition

Dual-rotor Configuration	Upstream Propeller	Downstream propeller	incoming flow velocity (m/s)	Rotational Speed (rpm)	Rotor Distance
Anti-rotor	CCW (Counter Clockwise)	CW(Clock-wise)	0,2,4,6	5000	0.2D - 1.2D
Co-rotor	CCW (Counter Clockwise)	CCW (Counter Clockwise)	0,2,4,6	5000	0.2D - 1.2D

IV. Measurement Results and Discussion

A. Aerodynamics force measurement results

The thrust measurement was conducted first for both anti-rotor and co-rotor configurations, while changing rotor distance and incoming flow velocity. To obtain a performance curve, the rotational speed was changed from 2000rpmto 7500rpm. Figure4 shows the thrust and power consumption curves of both the anti-rotor and co-rotor when the rotor distance was 0.6D and the incoming flow velocity was zero. For the anti-rotor, the total thrust generated by bothpropellers is about 55 percent higher than that of the isolated single rotor. The upstream propeller contributed 67 percent of the thrust, meaning that the performance of the upstream propeller was much better than that of the downstream propeller; this is reasonable because the local incoming flow velocity for the downstream propeller is higher and the incoming flow acts as a down-wash flow and decreases the local angle of attack, so the downstream propeller generates lower thrust. However, as concluded in the work of Shukle et al., the thrust of the upstream propeller of an anti-rotor is slightly higher than the isolated single propeller due to viscous swirl recovery by the counter-rotating lower rotor. For the co-rotor, the total thrust generated by both propellers is about 26 percent higher than that of an isolated single rotor.The upstream propeller contributes 80 percent of the thrust, indicating that the performance of the downstream propeller is worse than that of an anti-rotor. As described in the work of Theys et al.[16], this is mainly because the swirl losses can be minimized when using an anti-rotor. When using a co-rotor, the swirl losses would further affect the downstream propeller.

For the anti-rotor, the power consumption of both upstream and downstream propellers were basically the same, with the total power consumption double that of an isolated single propeller. For the co-rotor, since the downstream propeller generates smaller thrust, the power consumption is about 10 percent lower than for an isolated single propeller and an upstream propeller. When compared to an isolated single propeller, the co-rotor's total power consumption increased by 90%.

To investigate the influence of incoming flow velocity, we measured thrust and power consumption of both anti-rotor and co-rotor with incoming flow velocity values changing from $0 m/s$ to $6 m/s$. The thrust coefficient and power consumption coefficient were calculated using equation1 and equation2. Figure5 shows the thrust and power consumption coefficient of both anti-rotor and co-rotor for different rotor distance at a rotational velocity of 5000rpm. Regardless ofchanges in distance, the total anti-rotor thrust was 55 percent higher than that of the isolated single rotor, and the totalpower consumption was twice that of the isolated single propeller. For the co-rotor, the total thrust was 26 percent higher than for a single propeller, and the power consumption was 90 percent higher than for a single propeller. The rotor distance change does not affect this relationship. This test result shows that, contrary to intuition, for both anti-rotor and co-rotor the rotor distance change in the range of 0.2D to 1.2D does not much affect the thrust and power consumptionof the upstream and downstream propellers.

$$C_t = \frac{T}{\rho n^2 D^4} \tag{1}$$

$$C_P = \frac{P}{\rho n^3 D^5} \tag{2}$$

To compare performance of both anti-rotor and co-rotor under different incoming flow velocities, the advanced ratiocalculated by Equation 3 can be used to represent the incoming flow velocity.

$$J = \frac{U}{nD} \tag{3}$$

Figure 6 shows how the thrust coefficient and power consumption coefficient change with change of advanced ratio ofboth anti-rotor and co-rotor.For both anti-rotor and co-rotor, while the tendency of thrust and power coefficient, to decrease with an increase in incoming flow velocity, is the same as that of an isolated single propeller, the downwardtrend of lift and power of the downstream propeller is much less

than that for an isolated single propeller. When the incoming flow velocity is greater than 4m/s, the thrust generated by the upstream propeller even drops below that of the downstream propeller, showing that the disturbance of the upstream propeller to the incoming flow provides a kind of 'protection' for the downstream propeller, so that the downstream propeller is less affected by the incoming flow velocity. Such measurement results show that, although the performance of the downstream propeller is not as good asthe performance of a single propeller, when encountering a large incoming flow velocity, the downstream propeller maybe able to provide important thrust guarantees when the thrust of the upstream propeller is greatly reduced.

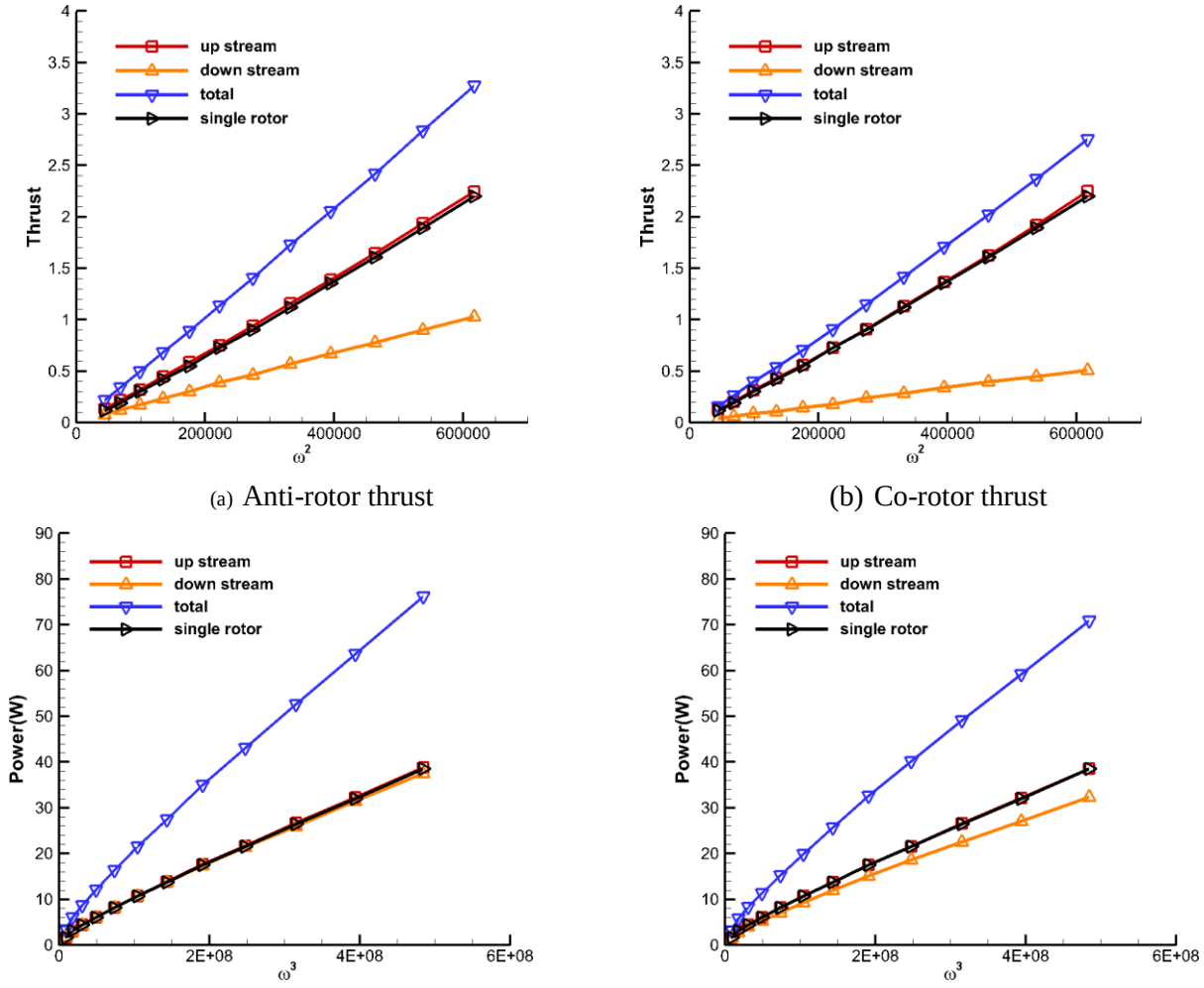

(a) Anti-rotor thrust (b) Co-rotor thrust

Anti-rotor power consumption (d) Co-rotor power consumption

Fig. 4 Thrust and power consumption measurement result of (a)(c) anti-rotor (b)(d) co-rotor with rotor distance $S = 0.6D$ and incoming flow velocity $U_\infty = 0$

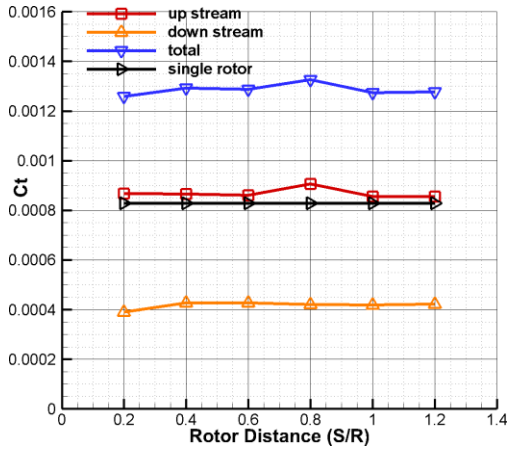

(a) C_t of anti-rotor

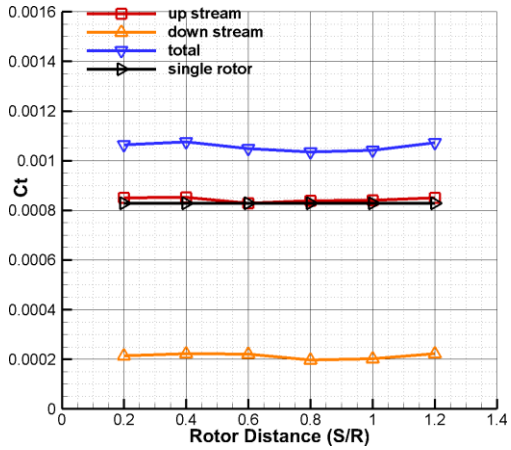

(b) C_t of co-rotor

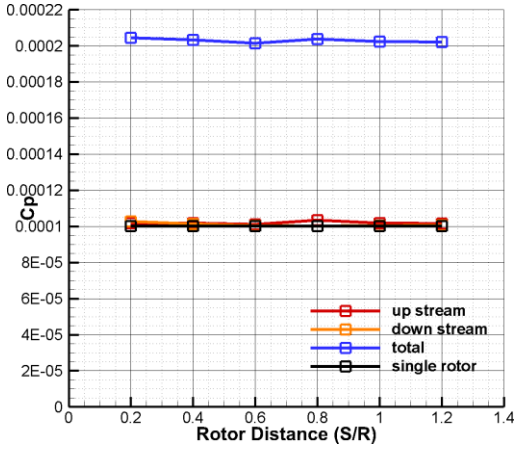

(c) C_p of anti-rotor

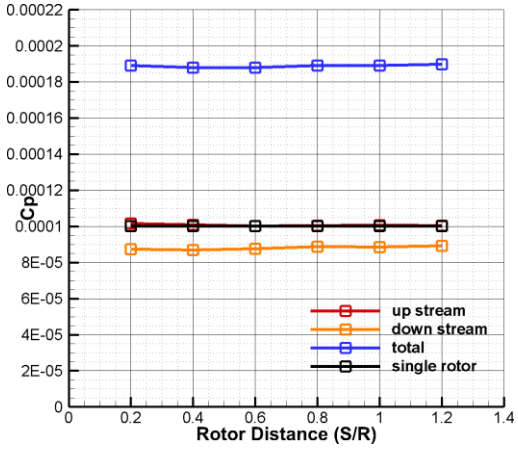

(d) C_p of co-rotor

Fig. 5 Thrust coefficient and power consumption coefficient of (a)(c) anti-rotor (b)(d) co-rotor with differentrotor distance. Incoming flow velocity $U_\infty = 0$, rotational speed $n = 5000rpm$

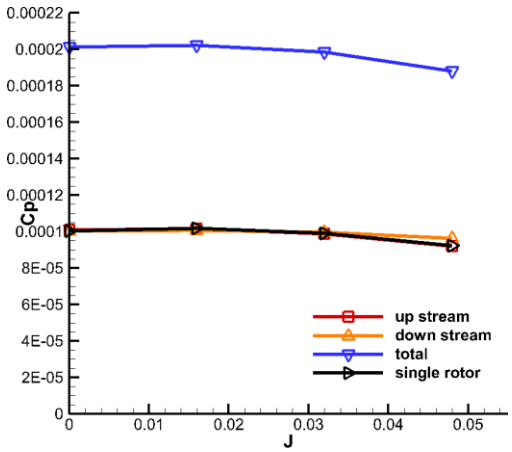

(a) C_t of anti-rotor

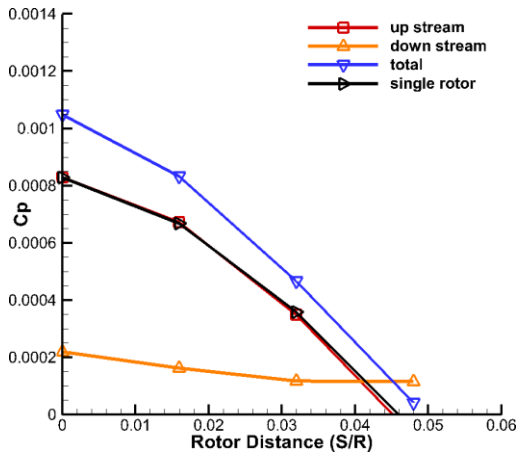

(b) C_t of co-rotor

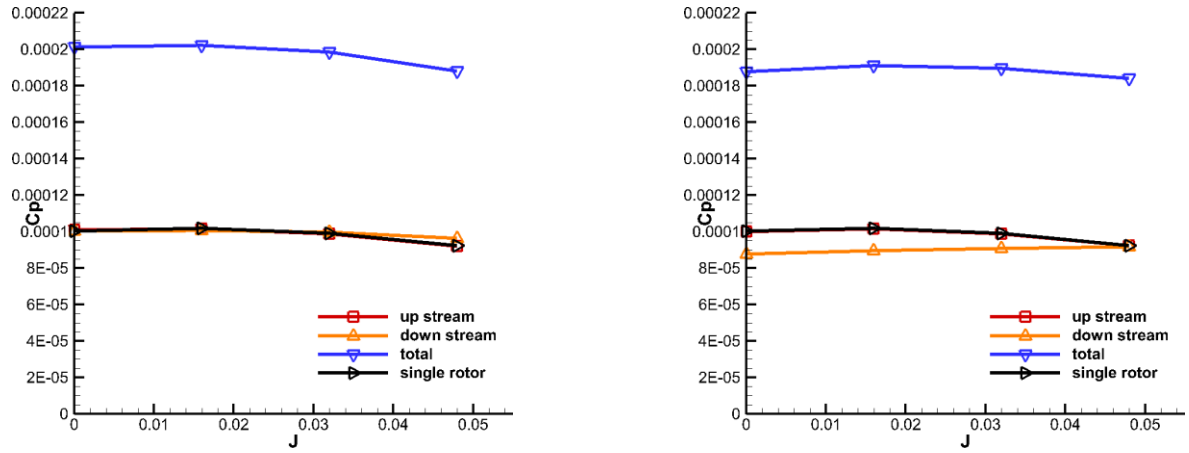

(c) C_p of anti-rotor (d) C_p of co-rotor

Fig. 6 Thrust coefficient and power consumption coefficient of (a)(c) anti-rotor (b)(d) co-rotor with differentadvanced ratio. Rotor distance $S = 0.6D$, rotational speed $n = 5000rpm$

B. flow field measurement results

To seek further understanding of the working conditions of the dual-rotor, as mentioned previously, a high-resolution particle imaging velocimetry (PIV) system was used to measure the flow field of both the anti-rotor and the co-rotor. Figure7the time-averaged flow field of the anti-rotor with a $0m\ s$ incoming flow velocity and a $5000rpm$ rotational speed. The X and Y axis are normalized based on the propeller diameter (240mm). The induced flow direction is alongthe positive direction of X axis. The air flow is accelerated after passing the upstream propeller, forming a flow field that shrinks toward the center of rotation. This is mainly because the air flow at the wing tip is slow, and the air flow at the center of the rotor is faster, and thus forming a relatively low pressure area. When the airflow passes the downstreampropeller, the speed is accelerated again, and the flow field once again undergoes a process of contracting from the wingtip to the center of rotation. The flow field of co-rotor is shown in Figure8. The shape of the flow field of co-rotoris very similar to the flow field of anti-rotor. But the acceleration of the downstream propeller to the airflow is slightlylower than that of the anti-rotating propeller. This also confirms the fact that the downstream propeller of co-rotor produces less thrust than the anti-rotor.

Figure9 shows the velocity distribution along the radial direction of a distance of 0.1D from the front and rear of the downstream anti-rotor propeller for different incoming flow velocities. For upstream flow of the downstream propeller,the velocity distribution at the outer part of the propeller is very similar, the only difference being that when the rotordistance is less than 0.2D, the incoming flow velocity of the part less than 0.3D is relatively low. This occurs becausewhen the rotor distance is 0.2D, and affected by the rotational center support structure, the flow field has not completely contracted to the center area. However, as the describes in work of Adkins et al.[24],since the central portions of the blades only contribute a small part of the thrust, the difference in the incoming flow velocity has no significant effecton the thrust performance of the downstream propeller. When the flow passes the downstream propeller, as shown inright column in Figure9, the velocity distribution of the flow field produced by the downstream propellers at different positions is almost the same. Such measurement results also confirm the previous test result, that the rotor distance overa range of 0.2D to 1.2D does not significantly affect the thrust generated by the downstream propeller.

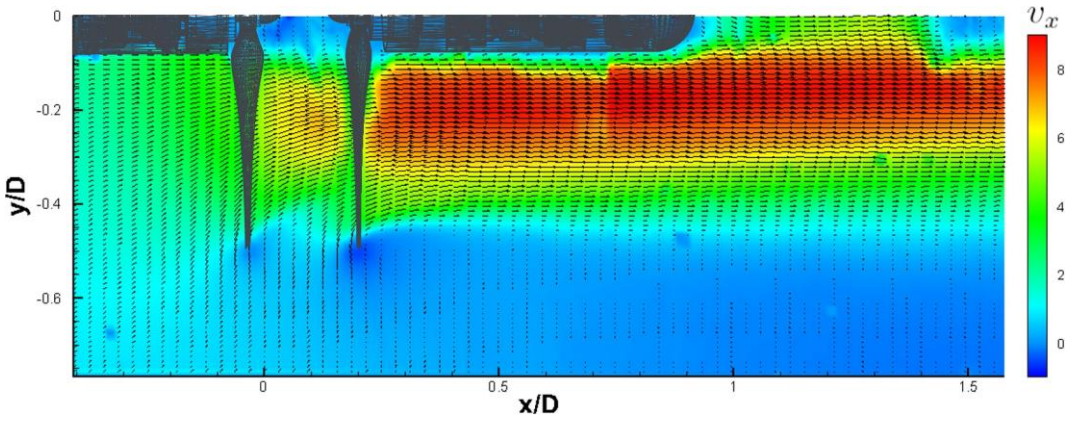

(a) Anti-rotor, $U_\infty = 0m/s$, $S = 0.2D$

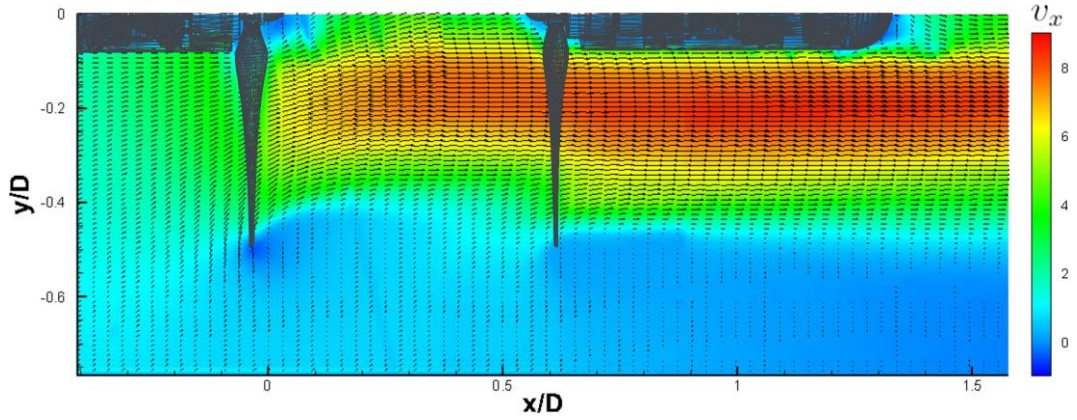

(b) Anti-rotor, $U_\infty = 0m/s$, $S = 0.6D$

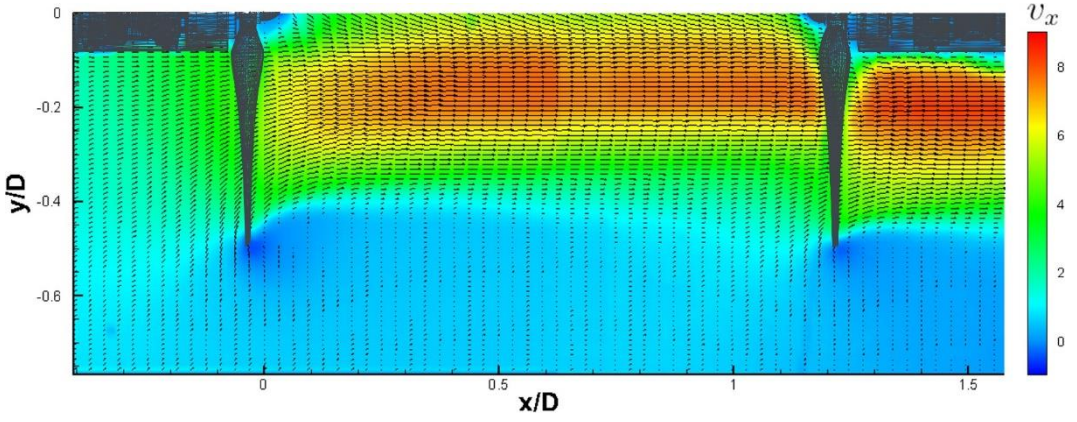

(c) Anti-rotor, $U_\infty = 0m/s$, $S = 1.2D$

Fig. 7 Time averaged velocity distribution of anti-rotor at hovering situation with rotor distance (a) $S = 0.2D$, (b) $S = 0.6D$, (c) $S = 1.2D$

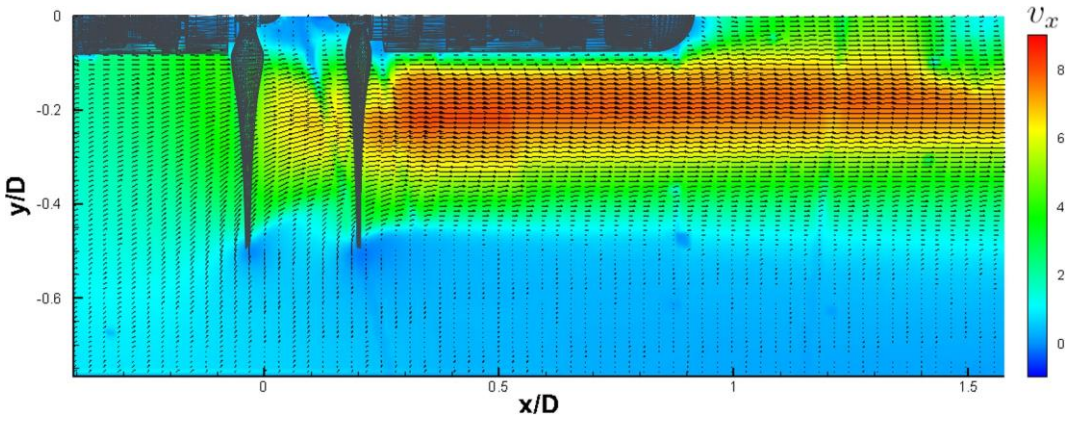

(a) Co-rotor, $U_\infty = 0m/s$, $S = 0.2D$

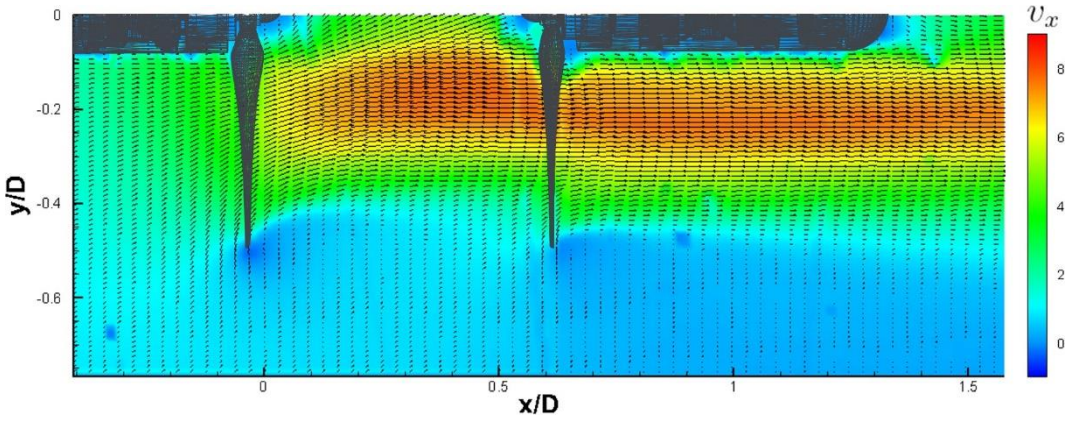

(b) Co-rotor, $U_\infty = 0m/s$, $S = 0.6D$

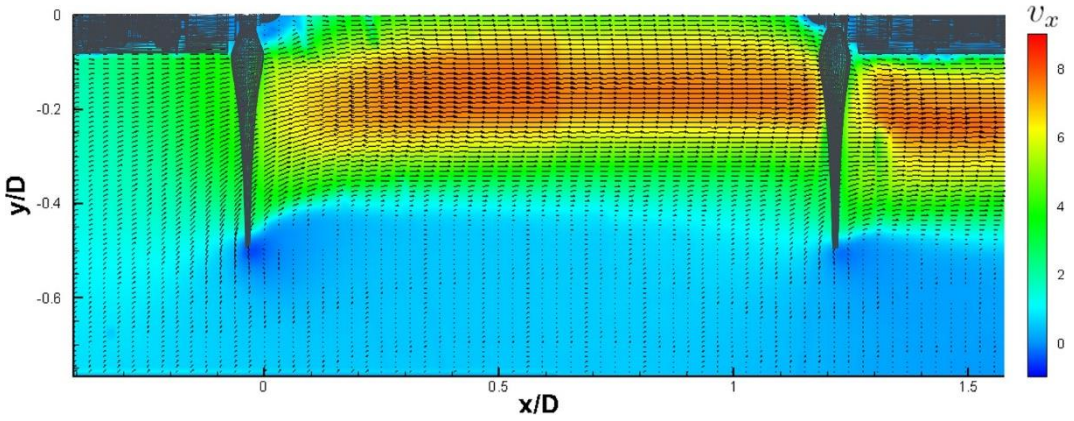

(c) Co-rotor, $U_\infty = 0m/s$, $S = 1.2D$

Fig. 8 Time averaged velocity distribution of co-rotor at hovering situation with rotor distance (a) $S = 0.2D$**, (b)**$\boldsymbol{S = 0.6D}$**, (c)** $\boldsymbol{S = 1.2D}$

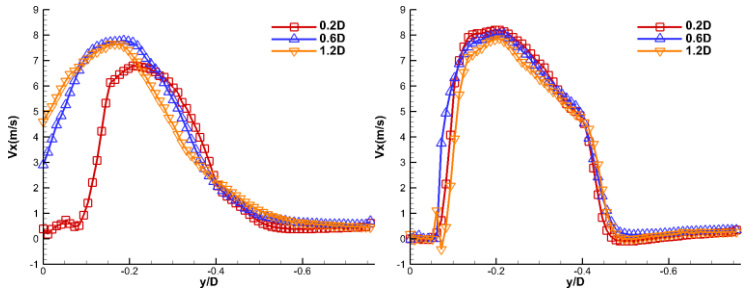

(a) $U = 0m/s$ (b) $U = 0m/s$

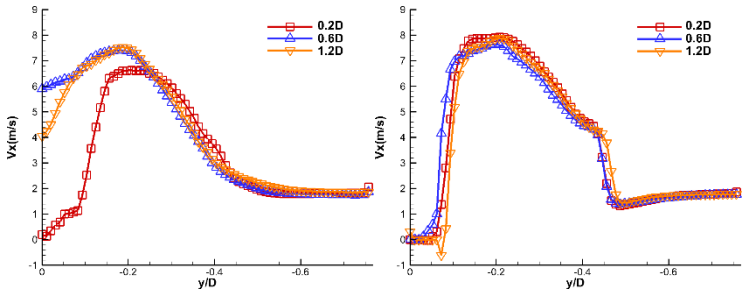

(c) $U = 2m/s$ (d) $U = 2m/s$

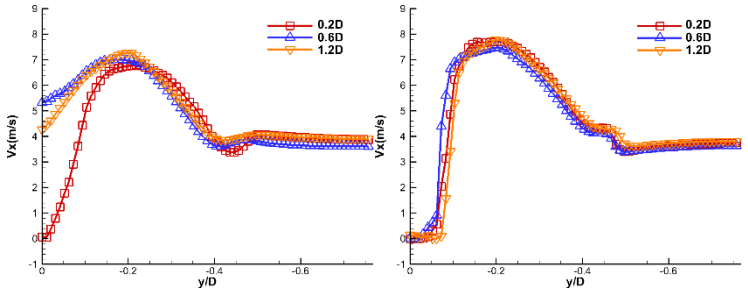

(e) $U = 4m/s$ (f) $U = 4m/s$

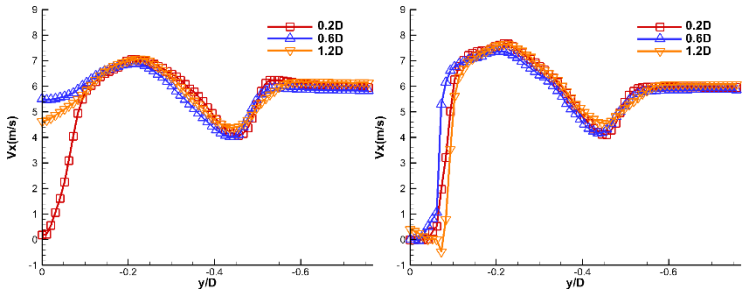

(g) $U = 6m/s$ (h) $U = 6m/s$

Fig. 9 X direction Velocity distribution along Y direction at (a)(c)(e)(g) $0.1D$ **before(left side) downstream propeller and (b)(d)(f)(h)** $0.1D$ **after(right side) downstream propeller under different incoming flow velocity, anti- rotor. Incoming flow velocity is (a)(b)** $0m/s$**, (c)(d)** $2m/s$**,(e)(f)** $4m/s$**,(g)(h)** $6m/s$**. Rotational speed** $n = 5000rpm$

Aero-acoustic measurement results

The noise generated by anti-rotor were measured for different rotational speeds and rotor distances. To separate the broadband noise signal, as described in the work of Blandeau et al. [25], a moving median filter was used for each frequency-domain signal. Figure 10shows a frequency domain and moving-filter using equation 4, where p is the sound pressure at one specific frequency, p_{ref} is the reference sound pressure equal to $2^{-5}\,pa$, f_0 is $50Hz$ and f_1 is $15000Hz$.

$$Ospl = 10log\frac{\int_{f_0}^{f_1} P^2 \cdot df}{p_{ref}^2} \tag{4}$$

The overall sound pressure level (OSPL) and overall sound pressure level of broadband noise ($OSPL_{BB}$) are shown in Figure11 showing that both the OSPL and the $OSPL_{BB}$ values increase with an increase of the propeller rotational speed. Compared with the single-rotor configuration, the anti-rotor configuration generated higher $OSPL_{BB}$ and the OSPL values, and OSPL and $OSPL_{BB}$ vary with rotor distance. as shown in Figure 12, this phenomenon exists at all the measurement positions.

The change of OSPL and $OSPL_{BB}$ with rotor distance is shown in Figure13, with both OSPL and $OSPL_{BB}$ increasing with increase of rotor distance. Since the previous test result shows that the thrust of neither upstream propeller or downstream propeller is affected by rotor distance, based on the description of aerodynamic noise in work of Blandeauet al[25], the harmonic noise should not be affected by the rotor distance because the thrust and torque do not change,so the main part of the noise change is the change in broadband noise. The measurement result is consistent with the prediction of Blandeau et al.[26]-which concluded that the main reason the bandwidth noise decreases with a reductionof rotor distance is that the integral length scale of the turbulence decreases significantly when the axial gap decreases.To confirm this explanation, the time averaged vortex distribution is calculated based on the flow field measurement. Figure14 shows the vortex distribution of the anti-rotor with $0m\ \ s$ incoming flow velocity. When the vortex intensity of the downstream propeller does not change significantly, increasing the distance between the rotors will significantly increase the interval in which the upstream propeller's wake vortex exists, thereby increasing the sound source of bandwidth noise, so the bandwidth noise would increase with an increase of the rotor distance.

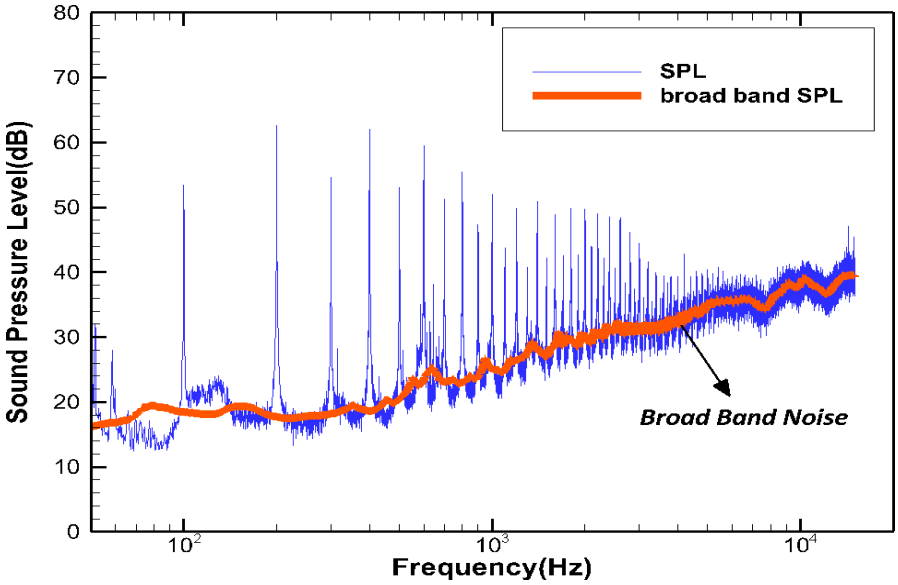

Fig. 10 Isolate broadband noise by media moving filter

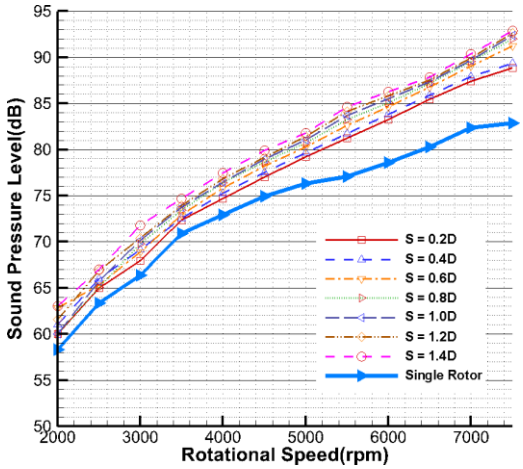

(a). Overall sound pressure level @β = 0°

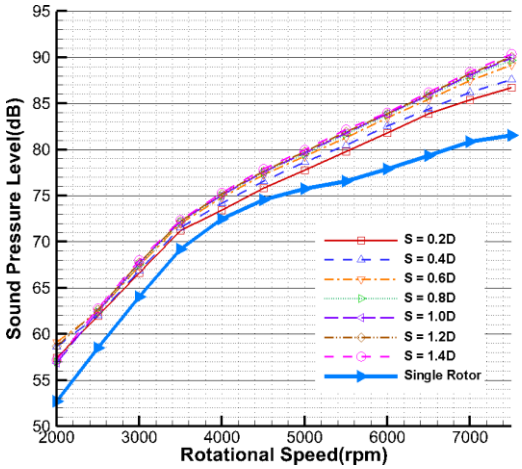

(b) Overall sound pressure level of broadband noise @β = 0°

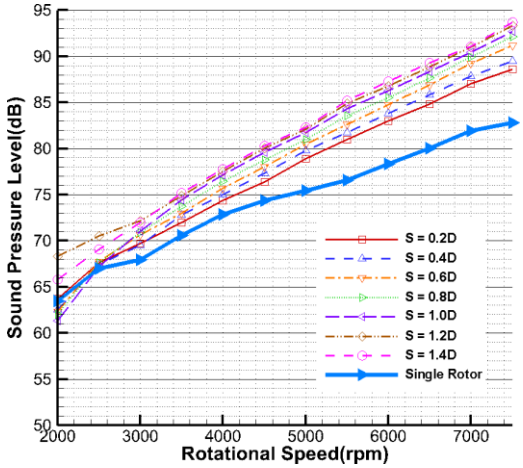

(c). Overall sound pressure level @β = 150°

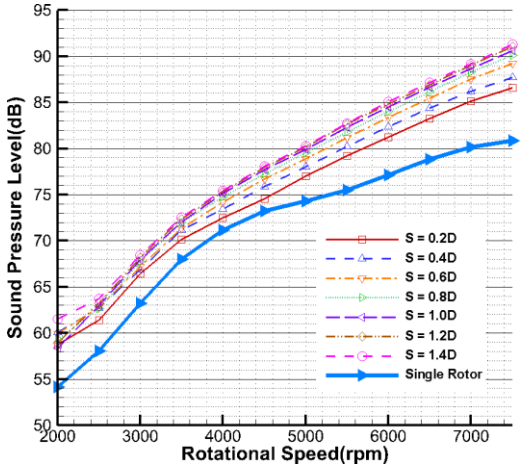

(d) Overall sound pressure level of broadband noise @β = 150°

Fig. 11 Overall sound pressure level and overall sound pressure level of broadband noise at position angle (a)(b) β = 0°, (c)(d) β = 150°

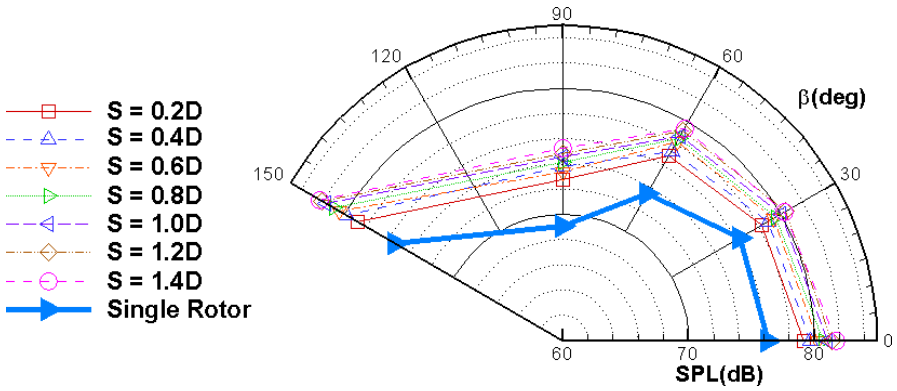

(a) Overall sound pressure level

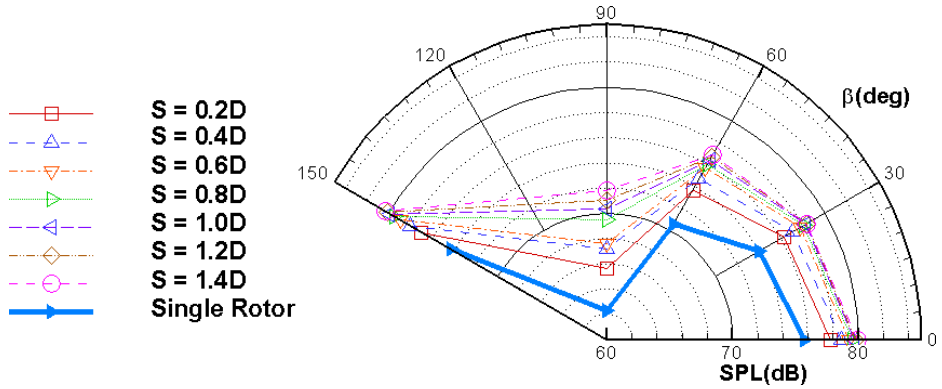

(b) Broad band sound pressure level

Fig. 12 Sound pressure level at different measurement position with rotational speed $5000r\ pm$

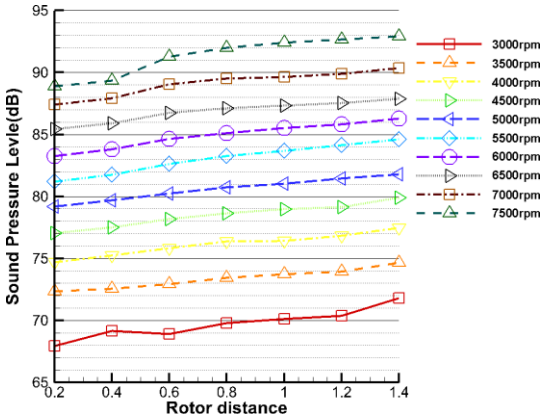

(a) $Os\ pl\ @\beta = 0^{\circ}$

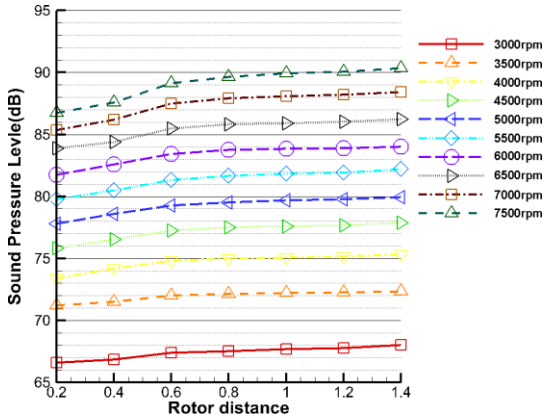

(b) $Os\ pl_{BB}\ @\beta = 0^{\circ}$

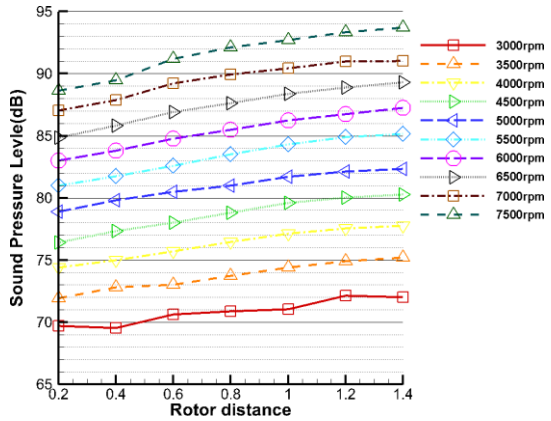

(c) $Os\ pl\ @\beta = 150^{\circ}$

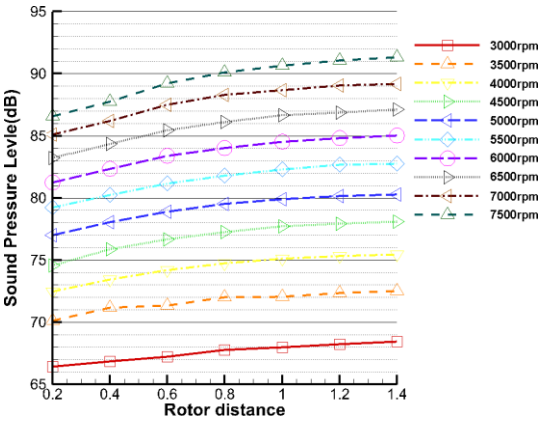

(d) $Os\ pl_{BB}\ @\beta = 150^{\circ}$

Fig. 13 Overall sound pressure level and overall sound pressure level of broadband noise changing with rotordistance at position angle (a)(b) $\beta = 0^{\circ}$**, (c)(d)** $\beta = 150^{\circ}$

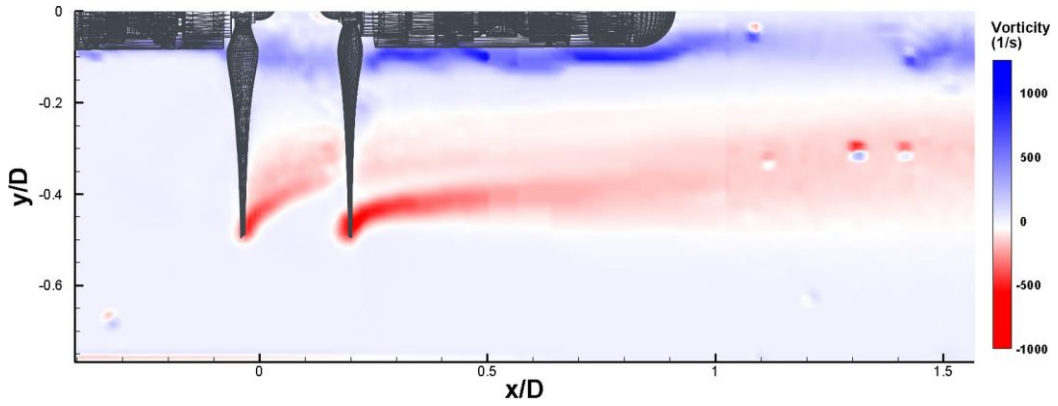

(a) Anti-rotor, $U = 0m/s$, $S = 0.2D$

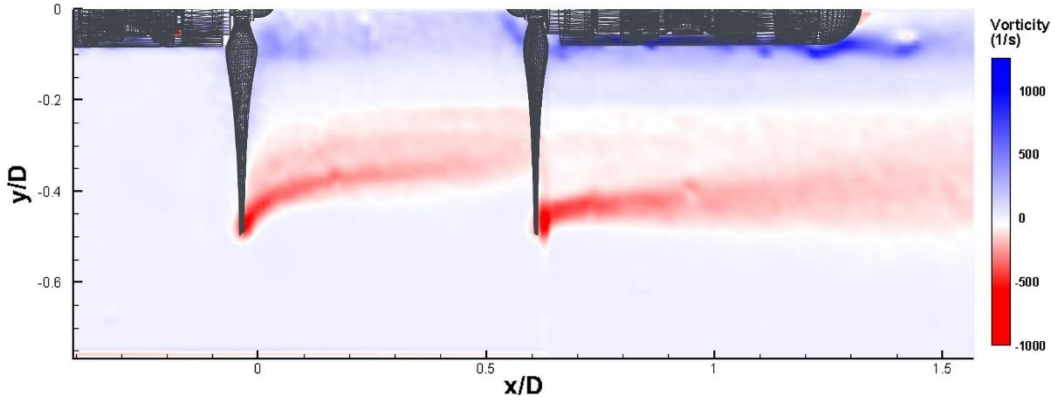

(b) Anti-rotor, $U = 0m/s$, $S = 0.6D$

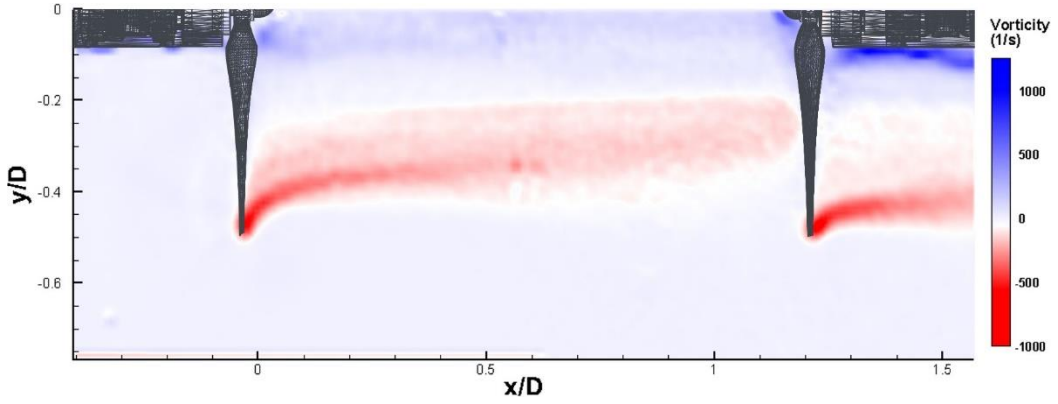

(c) Anti-rotor, $U = 0m/s$, $S = 1.2D$

Fig. 14 Time averaged vorticity distribution of anti-rotor at hovering situation with rotor distance (a) $S = 0.2D$**, (b)** $\boldsymbol{S = 0.6D}$**, (c)** $\boldsymbol{S = 1.2D}$

V. Conclusion

An experimental study on the aerodynamic and aeroacoustic performance of a dual-rotor configuration of a UAV propeller was conducted, and a parametric study of the effect of different rotor distances was performed. The flow fieldwas investigated by PIV measurement, and the noise level with respect to change of rotor distance was also measured.From the experiment results, it can be observed that:

Because swirl losses can be minimized using an anti-rotor, the anti-rotor could have better aerodynamic performance than that of a co-rotor, and the thrust performance of the downstream propeller will decrease

because it is affected by the upstream propeller's wake. Within a distance range between 0.2D to 1.2D, rotor distance has little effect on the overall aerodynamic performance of a dual rotor. The dual rotor generates a higher sound pressure level of broadband noise compared with that from an isolatedsingle rotor, with the noise decreasing as the distance between the rotors decreases. The research findings are believed to be very helpful in the design of UAV coaxial rotors and play a role in the development of more accurate prediction techniques for such systems.

Acknowledgments:

The research work is partially supported by Iowa Space Grant Consortium (ISGC) Base Program for Aircraft Icing Studies. The support of National Science Foundation (NSF) under award numbers of CBET-1916380 and CMMI-1824840 is also gratefully acknowledged.

References

[1] Siddique, M. A., Han, N., and Hu, H., "Development of an Experimental Unmanned-Aerial-System (UAS) to Study the Effectsof Adverse Weathers on its Flight Performance," *AIAA Science and Technology Forum and Exposition, AIAA SciTech Forum2022*, 2022. https://doi.org/10.2514/6.2022-1646, URL https://arc.aiaa.org/doi/abs/10.2514/6.2022-1646.

[2] "List of UAV applications," https://en.wikipedia.org/wiki/List_of_unmanned_aerial_vehicle_applications, 2014.

[3] Theys, B., Dimitriadis, G., Hendrick, P., and De Schutter, J., "Influence of propeller configuration on propulsion system efficiency of multi-rotor Unmanned Aerial Vehicles," *2016 International Conference on Unmanned Aircraft Systems (ICUAS)*, 2016, pp. 195–201. https://doi.org/10.1109/ICUAS.2016.7502520.

[4] Brandt, J., and Selig, M., "Propeller Performance Data at Low Reynolds Numbers," *49th AIAA Aerospace Sciences Meetingincluding the New Horizons Forum and Aerospace Exposition*, American Institute of Aeronautics and Astronautics, Reston, Virigina, 2011. https://doi.org/10.2514/6.2011-1255, URL http://arc.aiaa.org/doi/10.2514/6.2011-1255.

[5] Merchant, M., and Miller, L. S., "Propeller Performance Measurement for Low Reynolds Number UAV Applications," *44thAIAA Aerospace Sciences Meeting and Exhibit*, Vol. 18, American Institute of Aeronautics and Astronautics, Reston, Virigina, 2006, pp. 13695–13707. https://doi.org/10.2514/6.2006-1127, URL http://arc.aiaa.org/doi/10.2514/6.2006-1127.

[6] Ko, A., Ohanian, O. J., and Gelhausen, P., "Ducted Fan UAV modeling and simulation in preliminary design," *Collection ofTechnical Papers - 2007 AIAA Modeling and Simulation Technologies Conference*, Vol. 1, American Institute of Aeronautics and Astronautics Inc., 2007, pp. 161–180. https://doi.org/10.2514/6.2007-6375, URL https://arc.aiaa.org/doi/abs/10.2514/6.2007-6375.

[7] Ning, Z. "An experimental investigation on the dynamic ice accretion process and its effects on the aeromechanic performance of drone propellers," Ph.D. thesis, Iowa State University, 2020.

[8] Dhwanil Shukla, N. K., "Drone Scale Coaxial Rotor Aerodynamic Interactions Investigation," 2019. https://doi. org/10.1115/1.4042162,.

[9] Nagashima, T., and Nakanishi, K., "Optimum performance and wake geometry of co-axial rotor in hover," 1981.

[10] Zimmer, H., "The aerodynamic calculation of counter rotating coaxial rotors," 1985.

[11] Qi, H., Xu, G., Lu, C., and Shi, Y., "A study of coaxial rotor aerodynamic interaction mechanism in hover with high-efficienttrim model," *Aerospace Science and Technology*, Vol. 84, 2019, pp. 1116–1130.

[12] Harrington, R. D., "Full-scale-tunnel investigation of the static-thrust performance of a coaxial

helicopter rotor," Tech. rep., NATIONAL AERONAUTICS AND SPACE ADMINISTRATION WASHINGTON DC, 1951.

[13] Dingeldein, R. C., "Wind-tunnel Studies of the Performance of Multirotor Configurations," 1954.

[14] Hoffmann, G., Huang, H., Waslander, S., and Tomlin, C., "Quadrotor helicopter flight dynamics and control: Theory and experiment," *AIAA guidance, navigation and control conference and exhibit*, 2007, p. 6461.

[15] Bristeau, P.-J., Martin, P., Salaün, E., and Petit, N., "The role of propeller aerodynamics in the model of a quadrotor UAV,"

2009 European control conference (ECC), IEEE, 2009, pp. 683–688.

[16] Theys, B., Dimitriadis, G., Hendrick, P., and De Schutter, J., "Influence of propeller configuration on propulsion system efficiency of multi-rotor unmanned aerial vehicles," *2016 international conference on unmanned aircraft systems (ICUAS)*, IEEE, 2016, pp. 195–201.

[17] Ditmer, M. A., Vincent, J. B., Werden, L. K., Tanner, J. C., Laske, T. G., Iaizzo, P. A., Garshelis, D. L., and Fieberg, J. R., "Bears Show a Physiological but Limited Behavioral Response to Unmanned Aerial Vehicles," *Current Biology*, Vol. 25, No. 17, 2015, pp. 2278–2283.

[18] Glegg, S., and Devenport, W., *Aeroacoustics of low Mach number flows: fundamentals, analysis, and measurement*, Academic Press, 2017.

[19] Kurtz, D., and Marte, J., "A review of aerodynamic noise from propellers, rotors, and lift fans," 1970.

[20] Ning, Z., and Hu, H., "An experimental study on the aerodynamics and aeroacoustic characteristics of small propellers," *54thAIAA Aerospace Sciences Meeting*, 2016, p. 1785.

[21] Ning, Z., and Hu, H., "An experimental study on the aerodynamic and aeroacoustic performances of a bio-inspired UAV propeller," *35th AIAA Applied Aerodynamics Conference, 2017*, American Institute of Aeronautics and Astronautics Inc, AIAA, 2017. https://doi.org/10.2514/6.2017-3747, URL https://arc.aiaa.org/doi/abs/10.2514/6.2017-3747.

[22] Leslie, A., Wong, C., and Auld, D., "Acoustics and Sustainability: How should acoustics adapt to meet future demands? Broadband Noise reduction from a mini-UAV propeller through boundary layer tripping," Tech. rep., 2008.

[23] Han, N., Hu, H., and Hu, H., "An Experimental Investigation on the Dynamic Ice Accretion Process over the Blade Surface of a Rotating UAV Propeller." *AIAA Science and Technology Forum and Exposition, AIAA SciTech Forum 2022*, 2022. https://doi.org/10.2514/6.2022-1538, URL https://arc.aiaa.org/doi/abs/10.2514/6.2022-1538.

[24] Adkins, C. N., and Liebeck, R. H., "Design of optimum propellers," *Journal of Propulsion and Power*, Vol. 10, No. 5, 1994, pp. 676–682.

[25] Blandeau, V., "Aerodynamic Broadband Noise from Contra-Rotating Open Rotors," 2011, pp. 1–185.

[26] Blandeau, V. P., and Joseph, P. F., "Broadband Noise Due to Rotor-Wake/Rotor Interaction in Contra-Rotating Open Rotors,"*AIAA JOURNAL*, Vol. 48, No. 11, 2010. https://doi.org/10.2514/1.J050566.